

Sinusoidal-wavelength-scanning interferometer with double feedback control for real-time distance measurement

Osami Sasaki, Kazuhiro Akiyama, and Takamasa Suzuki

In addition to a conventional phase α the interference signal of a sinusoidal-wavelength-scanning interferometer has a phase-modulation amplitude Z_b that is proportional to the optical path difference L and amplitude b of the wavelength scan. L and b are controlled by a double feedback system so that the phase α and the amplitude Z_b are kept at $3\pi/2$ and π , respectively. The voltage applied to a device that displaces a reference mirror to change the optical path difference becomes a ruler with scales smaller than a wavelength. Voltage applied to a device that determines the amplitude of the wavelength scan becomes a ruler marking every wavelength. These two rulers enable one to measure an absolute distance longer than a wavelength in real time. © 2002 Optical Society of America

OCIS codes: 120.3180, 120.5050, 120.5060.

1. Introduction

Real-time distance measurement with a laser interferometer is important in applications such as semiconductor-wafer positioning, disk-drive calibration, and machine-tool control. Many instruments for measuring interferometric distance take a relative distance measurement with a single-wavelength interferometer. If there are short interruptions in the optical path, the relative distance measurement ends in failure. Many applications for distance metrology require absolute distance measurements. To meet this requirement, two-wavelength interferometers equipped with a function of real-time measurement have been developed. For real-time measurement, electronic circuits are employed to process two interference signals instead of computer processing. The unique techniques of real-time electronic processing in heterodyne interferometry and sinusoidal-phase-modulating interferometry were reported in Refs. 1 and 2, respectively. Recently wavelength-scanning interferometers with a wide scanning width of ~ 10 nm have been applied to ab-

solute distance measurement. In Ref. 3 linear wavelength scanning was used in heterodyne interferometry to obtain a wide range and high accuracy in the measurement. In Ref. 4 sinusoidal wavelength scanning was used in sinusoidal-phase modulating interferometry. However, measurement accuracy and the range of the interferometer in Ref. 4 were not sufficient for practical applications.

In this paper we employ the same sinusoidal-wavelength-scanning interferometer by using a superluminescent diode as in Refs. 4 and 5 and propose interference signal processing with feedback controls to obtain a high accuracy of several nanometers. In sinusoidal-phase-modulating interferometers the conventional phase α of the interference signal can be easily locked at a constant value as reported in Ref. 6, and the amplitude of sinusoidal wavelength scanning can be precisely controlled as reported in Ref. 4. These two advantages are utilized in the interferometer proposed here. In addition to phase α , the interference signal of the sinusoidal-wavelength-scanning interferometer has a modulation amplitude Z_b that is proportional to the optical path difference (OPD) and amplitude of the wavelength scan. First phase α is kept at a constant value of $3\pi/2$ by controlling the position of the reference mirror or the OPD with a feedback system. The OPD changes from the initial value of L to $L_z = L - L_{\alpha} = 3\lambda_0/4 + m\lambda_0$, where λ_0 is the central wavelength and m is an integer. Next the voltage V_b , which determines the amplitude of the wavelength scan, is controlled with a feedback system

The authors are with the Faculty of Engineering, Niigata University, 8050 Ikarashi 2, Niigata-shi 950-2181, Japan. O. Sasaki's e-mail address is osami@eng.niigata-u.ac.jp.

Received 31 October 2001; revised manuscript received 28 February 2002.

0003-6935/02/193906-05\$15.00/0

© 2002 Optical Society of America

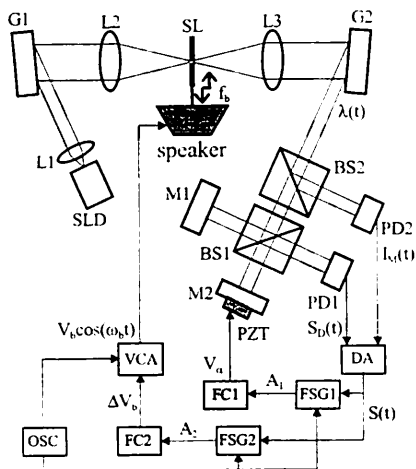


Fig. 1. SWS interferometer for real-time distance measurement: BS1, BS2, beam splitters; DA, divider; OSC, oscillator.

so that the modulation amplitude Z_b is kept at π for an OPD of L_z . Discrete values of the voltage V_b exist as stable points in the feedback control according to integer values of m . Therefore the stable points of the voltage V_b become a ruler marking every wavelength. Voltage applied to a piezoelectric transducer (PZT) that causes a change L_α in the OPD becomes a ruler with scales smaller than a wavelength. An OPD L longer than a wavelength can be measured accurately with two rulers in real time. A great advantage is that the ruler marking every wavelength can be calibrated automatically with double feedback control by changing the OPD at intervals of approximately a wavelength.

2. Interference Signal

Figure 1 shows the setup of the interferometer. We explain the kind of interference signal that is obtained in the sinusoidal-wavelength-scanning (SWS) interferometer by using a superluminescent laser diode (SLD). The output beam from the SLD is collimated with lens L1 and incident on diffraction grating G1. The first-order reflection from the grating is Fourier transformed with lens L2 to obtain the continuous spectrum of the SLD that appears on the focal plane of lenses L2 and L3. The central wavelength of the spectrum is λ_0 . Slit SL is placed on the focal plane, and a portion of the spectrum is transmitted. The slit is connected to the magnetic coil of a speaker and vibrates sinusoidally with an angular frequency of ω_b . The central wavelength of the light passing through the slit is sinusoidally scanned and expressed as

$$\lambda(t) = \lambda_0 + b \cos(\omega_b t). \quad (1)$$

The light coming from the slit is Fourier transformed with lens L3 and is incident on grating G2 so that the first-order reflection from the grating produces a collimated beam whose propagating direction is constant for all wavelengths contained in the spectrum of the SLD. The collimated beam becomes the out-



Fig. 2. Block diagram of feedback signal generator 1: MA, multiplier; LF, low-pass filter.

put of a SWS light source for an interferometer. The time-varying intensity of the collimated beam is denoted by $I_M(t)$, which is detected by photodiode PD2.

The output beam from the SWS light source is divided into two beams. One of them is reflected by an object. The other is reflected by reference mirror M2, which is displaced by the PZT. Interference signal $S_D(t)$ detected with photodiode PD1 is divided by intensity $I_M(t)$ to obtain an interference signal as follows:

$$S(t) = S_D(t)/I_M(t) = A + B \cos(Z_b \cos \omega_b t + \alpha), \quad (2)$$

where A and B are constants,

$$Z_b = (2\pi b/\lambda_0^2)L, \quad (3)$$

$$\alpha = -(2\pi/\lambda_0)L, \quad (4)$$

where L is an OPD.

3. Measurement Principle

A. Measurement of L_α with Feedback Control

We now explain how to measure a fractional value of OPD L by feedback control. The construction of the feedback signal generator, FSG1, is shown in Fig. 2. Multiplier MA multiplies signal $S(t)$ with $\cos(2\omega_b t)$, and the output of MA is fed to low-pass filter LF whose cutoff frequency is $(\omega_b/2\pi)/10$ to obtain a feedback signal,

$$A_1 = B J_2(Z_b) \cos \alpha = g \cos \alpha, \quad (5)$$

where J_2 is the second-order Bessel function. Feedback controller FC1 produces voltage V_α applied to the PZT. The feedback system controls the position of reference mirror M2 or the OPD so that the feedback signal A_1 becomes zero. The speed of the feedback control is determined mainly by the cutoff frequency of the low-pass filter, LF, in the feedback signal generator, FSG1. A change in the OPD caused by this feedback control is illustrated in Fig. 3.

In Fig. 3 negative feedback works in the region

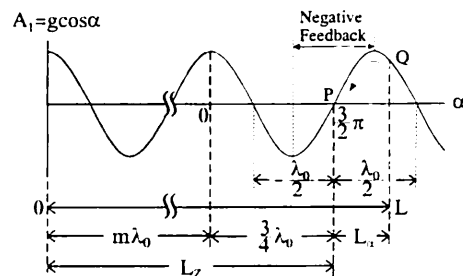


Fig. 3. Change in the OPD by feedback control, which keeps phase α at $3\pi/2$.

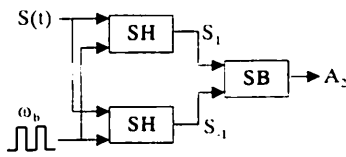


Fig. 4. Block diagram of feedback signal generator 2: SH, sample holder; SB, subtractor.

where the differential coefficient of A_1 with respect to α is positive, and the positive feedback works in the region where the differential coefficient is negative. First the OPD is at L and the position of signal A_1 is at point Q. The position of signal A_1 is moved to a stable point, P, by feedback control. Phase α becomes $3\pi/2 + 2m\pi$, where m is an integer. In Fig. 3 the value of L_α is positive when the first OPD L changes to a smaller OPD L_z by movement of the reference mirror, M2. L_α is a fractional value of the OPD L to be measured. The OPD at the stable point of the feedback control is given by

$$L_z = L - L_\alpha = 3\lambda_0/4 + m\lambda_0. \quad (6)$$

It is assumed that the first position, Q, of signal A_1 is at a point at which a negative value of signal A_1 is very small in the positive feedback region. In this case it is unclear whether the position moves to the right-hand side in Fig. 3, because sometimes noise contained in signal A_1 pulls the position to the left side. When the position of signal A_1 moves to the left side, the value of L_α exceeds $\lambda_0/2$. The same situation occurs when the first position, Q, of signal A_1 is at a point at which a positive value of signal A_1 is very small in the positive feedback region. Therefore the range of L_α is approximately between $-\lambda_0/2$ and $\lambda_0/2$. If an initial condition is given in which $L_\alpha = 0$ at $V_\alpha = 0$, L_α can be obtained by measuring the applied voltage V_α from the relationship of $L_\alpha = \beta V_\alpha$, where β is a constant. Its measurement accuracy is of the order of nanometers.

B. Measurement of L_z with Feedback Control

We explain how to measure an integer multiple of the wavelength in the OPD L . Since the phase α is kept at $3\pi/2$ by feedback control, the interference signal is

$$S(t) = A - B \sin(Z_b \cos \omega_b t), \quad (7)$$

where

$$Z_b = (2\pi b/\lambda_0^2)L_z. \quad (8)$$

The construction of feedback signal generator FSG2 is shown in Fig. 4. Signal $S(t)$ is sampled with sample holders, SHs, when $\cos \omega_b t = 1$ and $\cos \omega_b t = -1$ so that signals $S_1 = A - B \sin Z_b$ and $S_{-1} = A + B \sin Z_b$ are obtained. From these signals a feedback signal

$$A_2 = S_{-1} - S_1 = 2B \sin Z_b \quad (9)$$

is generated. A feedback controller, FC2, produces voltage ΔV_b that is fed to the voltage control ampli-

fier, VCA, and determines the amplitude V_b of the voltage applied to the speaker. The feedback system controls the amplitude V_b or the amplitude b of the wavelength scanning so that the signal A_2 becomes zero. This makes modulation amplitude Z_b equal to π . Then we have

$$b = \lambda_0^2/2L_z = 2\lambda_0/(4m + 3). \quad (10)$$

The values of b are discrete, corresponding to the values of m . Since amplitude b is proportional to amplitude V_b with a form of $b = D_1 V_b + D_0$, the values of V_b are also discrete. These discrete values of the amplitude V_b at which Z_b is equal to π are referred to as stable points of V_b .

The measured value of b is obtained from the measured value of V_b , and the measured value of L_z is calculated by the relationship of $L_z = \lambda_0^2/2b$. Since L_z is given in Eq. (6), the following value is calculated by using the measured value of L_z :

$$m_c = (L_z - 3\lambda_0/4)/\lambda_0. \quad (11)$$

Integer m can be decided by rounding off the value of m_c to an integer if a measurement error of L_z is smaller than $\lambda_0/2$. Finally the OPD is calculated with

$$L = 3\lambda_0/4 + m\lambda_0 + L_\alpha. \quad (12)$$

Note that once the relationship between the integer values of m and the stable points of V_b is given, the OPD can be obtained directly from Eq. (12) without calculating m_c . This means that the stable points of V_b are regarded as a ruler marking every wavelength, and the voltage V_α is regarded as a ruler with scales smaller than a wavelength. The calibration of the ruler produced by the voltage V_b can be made automatically by double feedback control by changing the OPD at intervals of approximately a wavelength.

4. Experiment

An interferometer for real-time distance measurement shown in Fig. 1 has been constructed. The central wavelength λ_0 and the spectral bandwidth of the SLD were 788.7 and 20 nm, respectively. A 1200-line/mm holographic grating was used for G1 and G2. The focus length of lenses L1 and L2 was 25 mm, and the width of slit SL was $\sim 100 \mu\text{m}$. The angular frequency of $\omega_b/2\pi$ was 400 Hz.

Mirror M1 fixed on a stage was used as an object. We displaced the object with a micrometer to change the OPD. By increasing the OPD at intervals of approximately one wavelength, we could move a stable point of V_b to the next point sequentially. We obtained 83 stable points of V_b whose order is denoted by the number N of 0–82, as shown in Fig. 5. The stability of the stable points with time is shown in Fig. 6. The numbers of the stable points are $N = 1-3$ in Fig. 6(a) and $N = 80-82$ in Fig. 6(b). The difference between two values of V_b at the adjacent stable points becomes smaller as the number N increases. In Fig. 6(a) it is easy to distinguish the

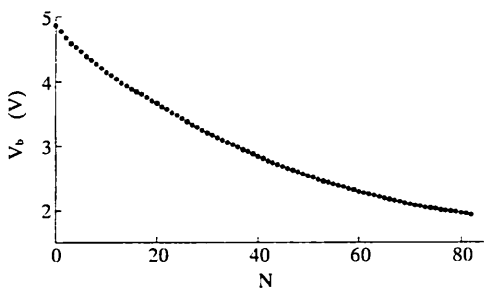


Fig. 5. Stable points of V_b .

three stable points. The maximum value of V_b depends on the spectral bandwidth of the SLD. It is 4.86 V at $N = 0$. Figure 6(b) shows the limit in distinguishing the three stable points. The minimum value of V_b is 1.93 V at $N = 82$.

We need the relationship between b and V_b to convert the measured value of V_b into a value of b . We explain how to obtain the relationship from the interference signal given by Eq. (7), in which the feedback control of V_b does not work. First we fixed the value of V_b and detected the interference signal given by Eq. (7). We calculated the value of Z_b from the interference signal with a computer by the method of sinusoidal-phase-modulating interferometry described in Ref. 7. By changing the OPD L , we found the relationship of $Z_b = \gamma L$. Since $\gamma = 2\pi b/\lambda_0^2$, we could calculate the value of b . Next we changed the value of V_b , and we obtained the relationship between b and V_b , as shown in Fig. 7. From this result the relationship of $b = 1.59V_b + 0.059$ was determined.

We tried to determine the integer m . We converted the stable points of V_b shown in Fig. 5 into values of b with the relationship $b = 1.59V_b + 0.059$ and obtained measured values of $L_z = \lambda_0^2/2b$. The values of m_c were calculated from the measured values of L_z by Eq. (11). Figure 8 shows the differences between the value of m_c and the integer of its round number. Since the absolute value of the difference

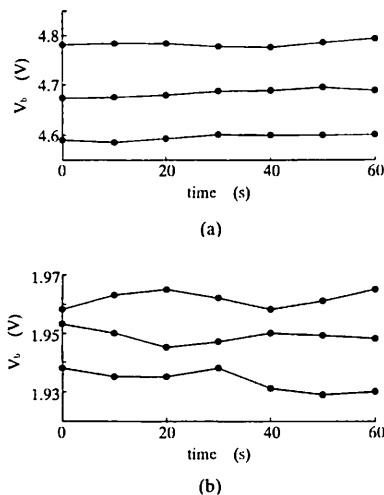


Fig. 6. Stability of the stable points with time: (a) $N = 1, 2,$ and $3,$ (b) $N = 80, 81,$ and $82.$

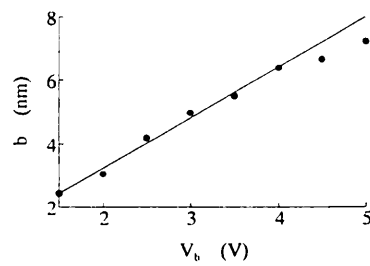


Fig. 7. Relationship between V_b and $b.$

was less than 0.5 in the region of $N = 20-70$, we could determine the values of integer m . From this result the relationship of $m = 46 + N$ was obtained.

Mirror M1 fixed on a stage was used as an object. Displacement D of the object with a micrometer changed the OPD at intervals of $\sim 5 \mu\text{m}$. We calculated the values of m_c from the measured values of V_b at the stable points by using the relationship $b = 1.59V_b + 0.059$. Measured results are shown at Table 1. The values of L_α were calculated with relationship $L_\alpha = \beta V_\alpha$, where $\beta = 83.37 \text{ nm/V}$. Since the measurement error in V_α was estimated to be less than 0.1 V, the measurement error in L_α or L was less than 8 nm. The differences between the value of m_c and an integer of its round number were within 0.03, which means that the measurement was carried out exactly.

Displacement D of the object with a micrometer changed the OPD at intervals of $\sim 10 \mu\text{m}$. Measured results are shown at Table 2. In this measurement we determined values of m by the relationship between the values of m and the stable points of V_b . Although many measured values of L_α were between $-\lambda_0/2$ and $\lambda_0/2$, we sometimes encountered measured values larger than $\lambda_0/2$. In Table 2 the measured value was 467 nm at $2D = 60 \mu\text{m}$. We confirmed that the measurement range was from 37

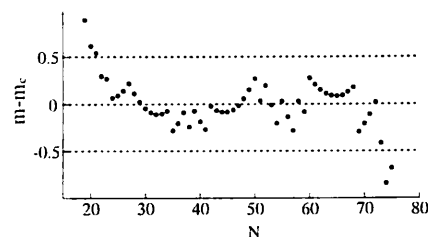


Fig. 8. Values of $m - m_c$ at the stable points of V_b shown in Fig. 5.

Table 1. Results of Measurements with a Value of b

$2D$ (μm)	V_b (V)	b (nm)	L_z (nm)	V_α (V)	L_α (nm)	m_c	L (nm)	ΔL (nm)
0	2.60	4.19	74799	-3.0	-250	93.69	74792	
5	2.43	3.92	79953	-3.1	-258	100.20	79536	4744
10	2.30	3.72	84400	-0.2	-17	105.82	84529	4994
15	2.17	3.51	89372	-2.0	-167	112.09	89131	4602
20	2.06	3.33	94060	2.1	175	118.01	94225	5094

Table 2. Results of Measurement with a Value of m

$2D$ (μm)	V_b (V)	m	V_α (V)	L_α (nm)	L (nm)	ΔL (nm)
0	4.77	47	-3.2	-267	37551	
10	3.92	60	1.8	150	48264	10713
20	3.32	73	-2.3	-192	58218	9954
30	2.80	87	1.8	150	69648	11430
40	2.46	99	3.3	275	79277	9629
50	2.17	112	3.6	300	89598	10321
60	1.98	125	5.6	467	100061	10463

to 102 μm in which the value of b changed from 8.3 to 3.1 nm. The measurement rate was ~ 20 Hz, which was determined by the cutoff frequency of the low-pass filter employed in the feedback control of V_α .

5. Conclusion

We have proposed a sinusoidal-wavelength-scanning interferometer in which the OPD and the amplitude of the sinusoidal wavelength scan are controlled by the double-feedback-control system. The voltage applied to the PZT that displaces the reference mirror and makes the phase α equal to $3\pi/2$ becomes a ruler with scales smaller than a wavelength. The voltage applied to the speaker that determines the amplitude of the wavelength scan and makes the amplitude Z_b equal to π becomes a ruler marking every wavelength. The ruler marking every wavelength could be calibrated automatically with double feedback

control by changing the OPD at intervals of approximately a wavelength. These two rulers enabled us to measure an absolute distance longer than a wavelength in real time. The measurement range was from 37 to 102 μm , and the measurement error was less than 8 nm. The measurement rate was ~ 20 Hz. Studies are now under way to improve these characteristics.

References

1. R. Onodera and Y. Ishii, "Two-wavelength laser-diode interferometer with fractional fringe techniques," *Appl. Opt.* **34**, 4740-4746 (1995).
2. T. Suzuki, K. Kobayashi, and O. Sasaki, "Real-time displacement measurement with a two-wavelength sinusoidal phase-modulating laser diode," *Appl. Opt.* **39**, 2646-2652 (2000).
3. X. Dai and K. Seta, "High-accuracy absolute distance measurement by means of wavelength scanning heterodyne interferometry," *Meas. Sci. Technol.* **9**, 1013-1035 (1998).
4. O. Sasaki, N. Murata, K. Akiyama, and T. Suzuki, "Sinusoidal wavelength-scanning interferometers using a superluminescent diode," in *Applications: Interferometry '99*, W. P. O. Jüptner and K. Paturski, eds., *Proc. SPIE* **3745**, 196-204 (1999).
5. O. Sasaki, N. Murata, and T. Suzuki, "Sinusoidal wavelength-scanning interferometer with a superluminescent diode for step-profile measurement," *Appl. Opt.* **39**, 4589-4592 (2000).
6. T. Suzuki, O. Sasaki, and T. Maruyama, "Phase-locked laser diode interferometry for surface profile measurement," *Appl. Opt.* **28**, 4407-4410 (1989).
7. O. Sasaki and H. Okazaki, "Sinusoidal phase modulating interferometry for surface profile measurement," *Appl. Opt.* **25**, 3137-3140 (1986).